JOURNAL OF Applied Polymer SCIENCE

# Special Issue: Bioactive Surface Functionalization

**Guest Editor:** Prof. Koon Gee Neoh (National University of Singapore)

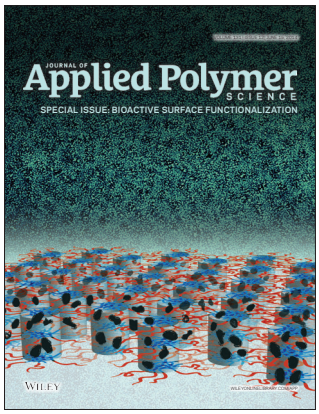



## EDITORIAL

**Bioactive Surface Functionalization**
K. G. Neoh, *J. Appl. Polym. Sci.* 2014, **DOI: 10.1002/app.40607**

## REVIEWS

**Orthogonal surface functionalization through bioactive vapor-based polymer coatings**
X. Deng and J. Lahann, *J. Appl. Polym. Sci.* 2014, **DOI: 10.1002/app.40315**

**Surface modifying oligomers used to functionalize polymeric surfaces: Consideration of blood contact applications**
M. L. Lopez-Donaire and J. P. Santerre, *J. Appl. Polym. Sci.* 2014, **DOI: 10.1002/app.40328**

**Block copolymers for protein ordering**
J. Malmström and J. Travas-Sejdic, *J. Appl. Polym. Sci.* 2014, **DOI: 10.1002/app.40360**

## RESEARCH ARTICLES

**MS-monitored conjugation of poly(ethylene glycol) monomethacrylate to RGD peptides**
O. I. Bol'shakov and E. O. Akala, *J. Appl. Polym. Sci.* 2014, **DOI: 10.1002/app.40385**

**Synthesis and characterization of surface-grafted poly(*N*-isopropylacrylamide) and poly(carboxylic acid)—Iron particles via atom transfer radical polymerization for biomedical applications**
J. Sutrisno, A. Fuchs and C. Evrensel, *J. Appl. Polym. Sci.* 2014, **DOI: 10.1002/app.40176**

**Deposition of nonfouling plasma polymers to a thermoplastic silicone elastomer for microfluidic and biomedical applications**
P. Gross-Kosche, S. P. Low, R. Guo, D. A. Steele and A. Michelmore, *J. Appl. Polym. Sci.* 2014, **DOI: 10.1002/app.40500**

**Regeneration effect of visible light-curing furfuryl alginate compound by release of epidermal growth factor for wound healing application**
Y. Heo, H.-J. Lee, E.-H. Kim, M.-K. Kim, Y. Ito and T.-I. Son, *J. Appl. Polym. Sci.* 2014, **DOI: 10.1002/app.40113**

**Bioactive agarose carbon-nanotube composites are capable of manipulating brain–implant interface**
D. Y. Lewitus, K. L. Smith, J. Landers, A. V. Neimark and J. Kohn, *J. Appl. Polym. Sci.* 2014, **DOI: 10.1002/app.40297**

**Preparation and characterization of 2-methacryloyloxyethyl phosphorylcholine (MPC) polymer nanofibers prepared via electrospinning for biomedical materials**
T. Maeda, K. Hagiwara, S. Yoshida, T. Hasebe and A. Hotta, *J. Appl. Polym. Sci.* 2014, **DOI: 10.1002/app.40606**

**Nanostructured polystyrene films engineered by plasma processes: Surface characterization and stem cell interaction**
S. Mattioli, S. Martino, F. D'Angelo, C. Emiliani, J. M. Kenny and I. Armentano, *J. Appl. Polym. Sci.* 2014, **DOI: 10.1002/app.40427**

**Microtextured polystyrene surfaces for three-dimensional cell culture made by a simple solvent treatment method**
M. E. DeRosa, Y. Hong, R. A. Faris and H. Rao, *J. Appl. Polym. Sci.* 2014, **DOI: 10.1002/app.40181**

**Elastic biodegradable starch/ethylene-co-vinyl alcohol fibre-mesh scaffolds for tissue engineering applications**
M. A. Susano, I. B. Leonor, R. L. Reis and H. S. Azevedo, *J. Appl. Polym. Sci.* 2014, **DOI: 10.1002/app.40504**

**Fibroblast viability and inhibitory activity against Pseudomonas aeruginosa in lactic acid–grafted chitosan hydrogels**
A. Espadín, N. Vázquez, A. Tecante, L. Tamay de Dios, M. Gimeno, C. Velasquillo and K. Shirai, *J. Appl. Polym. Sci.* 2014, **DOI: 10.1002/app.40252**

**Surface activity of pepsin-solubilized collagen acylated by lauroyl chloride along with succinic anhydride**
C. Li, W. Liu, L. Duan, Z. Tian and G. Li, *J. Appl. Polym. Sci.* 2014, **DOI: 10.1002/app.40174**

**Collagen immobilized PET-g-PVA fiber prepared by electron beam co-irradiation**
G. Dai, H. Xiao, S. Zhu and M. Shi, *J. Appl. Polym. Sci.* 2014, **DOI: 10.1002/app.40597**

JOURNAL OF Applied Polymer SCIENCE

# Nanostructured Polystyrene Films Engineered by Plasma Processes: Surface Characterization and Stem Cell Interaction

**Samantha Mattioli,[1] Sabata Martino,[2] Francesco D'Angelo,[2,4] Carla Emiliani,[2] Josè Maria Kenny,[1,3] Ilaria Armentano[1]**

[1]Materials Science and Technology Center, UdR INSTM, NIPLAB, Department of Civil and Environmental Engineering, University of Perugia, Terni, Italy

[2]Department of Chemistry, Biology and Biotechnologies, Biochemistry and Molecular Biology Unit, University of Perugia, Perugia, Italy

[3]Institute of Polymer Science and Technology, CSIC, Madrid, Spain

[4]Angelantoni Life Science s.r.l., Località Cimacolle, 464 06056, Massa Martana PG, Italy

Correspondence to: I. Armentano (E-mail: Ilaria.armentano@unipg.it)

**ABSTRACT:** In this work we showed the promising perspectives offered by the radiofrequency plasma processes on polymeric substrates. Polystyrene (PS) films with micropatterned grooves and nanostructured roughness were developed by Oxygen plasma treatment coupled with mask, and t process parameters, as power supply and treatment time were modulated. Then, hydrogenated amorphous carbon (a-C:H) coatings (~30 nm thickness) were deposited by methane radiofrequency plasma enhanced chemical vapor deposition (rf-PECVD) on the polymer surface. Oxygen modified PS surface showed improved wettability, roughness and etching rate by increasing the power supply and the treatment time. Uniform and patterned bi-layer films show a regular surface morphology, uniform chemical properties, with a contact angle to water of 77°, a surface energy of 51.15 mN $m^{-1}$ and good stability in physiological conditions. Nanoindentation measurements revealed a decrease of the bi-layer friction coefficient from 0.76 of PS to 0.17, highlighting the improvement of the nanomechanical properties of the novel developed system. Interaction with human bone-marrow mesenchymal stem cells demonstrates that uniform and patterned PS based films are biocompatible surfaces and remarkable, that groove patterned substrates induce stem cell alignment and elongation. © 2014 Wiley Periodicals, Inc. J. Appl. Polym. Sci. **2014**, *131*, 40427.

**KEYWORDS:** nanostructured polymers; surfaces and interfaces; biomedical applications

Received 15 October 2013; accepted 7 January 2014
**DOI: 10.1002/app.40427**

## INTRODUCTION

The demand for polymeric materials has been increasing and highly functionalized surface polymers are much desired to the production materials, for wider applications ranging from eco-friendly materials to biomaterials.

The surface properties of materials play a crucial role in biomedical applications[1,2] and the control of surface properties is very important for the high performance of adhesion, biomaterials and paints. Surface modification of polymers has been extensively employed to functionalize polymers by improving the surface properties such as adhesion, wetting, and biological compatibility, which can be controlled not only by the surface composition but also by the topography of the surface.[3]

Polystyrene (PS) has been used as a popular culture vessel for microbes due to its excellent durability, good optical properties and non-toxicity. The tissue culture polystyrene, as a standard *in vitro* cell culture substrate, is unsuitable for serum free cell culture medium since it normally occurs in a poor and insufficiently reproducible manner.[4] Therefore, surface modifications are required to optimize cell adhesion and accelerate the cell proliferation.

Glow discharge plasmas are generally used for the surface modification of polymers because the processes involved are solvent-free and dry, the consumption of chemicals is extremely low and need for sterilization of the products is eliminated. Moreover these processes are precisely controllable.[5] The surface can be treated homogeneously and the surface chemistry can be tailored for the required end use.[6] Glow discharge plasmas contain energetic neutrals, ions, and electrons, which act on a surface under treatment to change its physicochemical properties. The nature of the gas species used and the energy of the ions are important parameters, which can affect the properties of the polymer surface immersed in plasma.

By using plasma technique, we can perform three different processes: etching, deposition, and treatment on polymeric surface, without modifying bulk properties.

Amorphous carbon (a-C:H) films, which have been demonstrated to be biocompatible both *in vitro*[7–9] and *in vivo*[10] and to have many other desirable properties including excellent hardness, high stability, and favorable tribological properties,[11] can be deposited by plasma process. a-C:H coating is a very promising approach for improving the biomechanical properties of the polymer, since it should transfer its chemical inertness, hardness, wear resistant and biocompatibility to the polymer substrate.[11]

It is well-known that cell attachment in the first stage is controlled by the interaction between cell and material surface, while the longer term adhesion and proliferation are also associated with the presence of specific biological molecules and/or proteins.[12–15]

Surface design generating biomaterial nanotopography for tissue engineering–based strategies has been demonstrated to enhance differentiation of progenitor cells into their programmed lineage pathway.[16,17] To this aim, efforts have been made to tailor the surface of biomedical devices, and biomaterials in general, to provide chemical and physical cues to become biocompatible with the surrounding tissues or to guide cells to form tissue.[16] Many different cell types have been shown to respond to topographies of varying shapes and sizes, but little is known about stem cell behavior on smooth and nanopatterned surfaces.

In this work, surface treatment and deposition on polymeric substrate were analyzed and combined in order to develop biocompatible surfaces with modulated surface topography, low friction coefficient, good adhesion, and adequate surface properties for stem cell culture. The effect of the surface energy, topography, and nanomechanical properties on stem cell behavior was also reported.

This article focuses on the fabrication of nanostructured polymeric surfaces by means of different plasma processes and the investigation of the influence of process parameters on the morphological, chemical, wettability, mechanical and biocompatibility properties.

## EXPERIMENTAL

### Process of Polymeric Surface Nanotopography

Polystyrene (PS) was chosen for substrate fabrication, as it is a biocompatible polymer that is used extensively in cell culture experimentation.[18]

Polystyrene film deposition was performed by spin coating method by using a spin coater (Fr10KPA of CaLCTec instruments). Polymer was dissolved in toluene with concentration of 0.1 mg $mL^{-1}$, 200 μL of solution were placed on a clean glass cover slip with the rotation speed of 2000 rpm, for 30 s. The samples were dried at room temperature for 24 h, when the toluene was fully evaporated as previously reported.[19,20]

The PS films were treated by means of Oxygen ($O_2$) radiofrequency plasma method using a Sistec apparatus with a Huttinger power supply at 13.56 MHz. Power supply and treatment time, were used in order to study their effect on the surface properties and topography of the polymeric surfaces. The films were placed into the stainless steel chamber, and then it was evacuated for 1 h until the pressure reached $9 \times 10^{-3}$ Torr. The deposition condition was: power supply ranging from 5 to 30 W, pressure $9 \times 10^{-2}$ Torr, bias voltage ranging from 140 to 380 V and treatment time ranging from 2.5 to 30 min.

To develop specific PS grooves with different height, a mask, named 300P (with nominal microstructure of 300 grooves per inch) was selected and put onto the PS films during the plasma process, according to our previous work.[17]

### Uniform Film Characterization

The PS film thickness was measured using the reflection optical microscope NIS-elements BR software.

Static contact angle measurements were used to investigate the wettability and the surface energy of treated PS film. The contact angles were assessed using the sessile drop method in air using a FTA1000 Analyzer. Sterile water drops of 20 μL (high-performance liquid chromatography grade water) were placed on films, and measurements were recorded 10 s after the liquid made contact with the surface. Five independent determinations at different samples were averaged. The determination of surface energy was based on the Owens and Wendt method,[21] and two test liquids (deionized water and diiodomethane) were used as a probe for surface free-energy (S.E.) calculations.

### Nanopattern Characterization

Morphological analysis of PS patterned films was conducted using field emission scanning electron microscope (FESEM, Supra 25 Zeiss) on gold sputtered coated samples. Atomic force microscope (AFM, easy Scan AFM Nanosurf) was used to study the topography of the PS treated thin films. AFM images were recorded in a tapping mode at room temperature in air, using silicon cantilevers. The thickness and the uniformity of the films were investigated and quantified. The scan rate was 0.5 s/line.

### PS/a-C:H Bilayer Films

Bi-layer films were also designed and developed combining the etching effect of Oxygen plasma on PS surface and the amorphous carbon (a-C:H) thin film deposition.

The PS films were treated by means of Oxygen radiofrequency plasma method, as previously described. a-C:H film was deposited on uniform and patterned PS by using methane ($CH_4$) gas, power supply fixed at 15 W for 5 min. Patterned films were developed, in order to generate a chemical uniform grooves with the same heights reported in Process of Polymeric Surface Nanotopography section, but uniform chemistry due to a-C:H deposition.

Uniform films based on polystyrene were developed by spin coating, and surface modified by Oxygen plasma treatment and amorphous carbon deposition and named PSU, PSU+$O_2$, PSU+a-C:H respectively, while patterned bi-layer films were also developed by combining Oxygen plasma etching coupled with mask and amorphous carbon deposition, named PS+$O_2$+a-C:H.

The hardness and elastic modulus values of the films were determined by nanoindentation measurements by Nano Test nanoindenter of Micromaterials using a three-sided pyramidal diamond (Berkovich) indenter, with a load maximum of 5 mN,

with a loading/unloading rate of 0.2 mN $s^{-1}$ and dwell time 60 s. The NanoTest measures the penetration depth of the calibrated diamond indenter as a function of the applied load during a load–unload cycle. A series of 25 indentations were performed for each samples. Friction coefficients were also measured in the nanoscratch tests by using Rockwell indenter. The normal load of the scratch test was ramped from 0 to 5 mN. The scratch length was set to be 1000 μm. The lateral force was divided by the normal force to calculate the coefficient of friction of films. Ten scratch tests were conducted on each sample. Fourier infrared (FT-IR) spectra of PSU, PSU+$O_2$, PSU+a-C:H were also recorded using a Jasco FT-IR 615 spectrometer in the 400–4000 $cm^{-1}$ range, in attenuated reflectance (ATR) mode.

### Protein Adsorption

Protein adsorption assessments were performed by transferring 300 μg of bovine serum albumin (BSA, Sigma–Aldrich), 10% fetal bovine serum (FBS, Euroclone) culture medium, or plasma onto nanostructured polystyrene samples. Proteins were incubated for either 30 min or 24 h at 37°C (according to D'Angelo et al.[17]). After three washing steps in $H_2O$ total protein content was measured by the Bradford method[22] using BSA as the standard. Absorbance (595 nm) was measured using a microtiter plate reader (ELISA reader, GDV-DV990BV6, Italy). Every sample was analyzed in five independent experiments, each of which was triplicated. Data reported are the mean value ± standard error of the mean of each group.

### Stem Cell Interaction

**Isolation and Culture of Human Bone Marrow–Mesenchymal Stem Cells.** Human mesenchymal stem cells-bone marrow derived (hBM-MSCs) were isolated and cultured as previously described[17,23]; briefly, bone marrow cells were obtained from washouts of the medullary cavities of the femurs of informed patients undergoing primary total hip replacement.

Bone marrow was diluted with phosphate buffer saline (PBS) without $Ca^{2+}$/$Mg^{2+}$ plus EDTA, mononuclear cells were isolated by density gradient on Lympholyte® (Cedarlane Laboratories Limited) and seeded in 25-$cm^2$ culture flasks at a density of 2.5 × $10^6$ cells $mL^{-1}$ in control medium consisting of RPMI-1640 (Euroclone) medium containing 10% FBS, 2 m*M* of L-glutamine, and 100 U $mL^{-1}$ of penicillin–streptomycin (Euroclone) in a humidified atmosphere and 5% carbon dioxide ($CO_2$) at 37°C. After 5–7 days, the nonadherent cells were removed, and fresh medium was added to the flasks. After 15 days, a fibroblast-like colony started to grow. The medium was changed every 3 days.

Cultured hBM-MSCs were analyzed by flow cytometry for their surface marker expression. Cultured hBM-MSCs were tripsinized, washed and resuspended in PBS, supplemented with 1% bovine serum albumin and incubated with either FITC-, PE-, APC conjugated monoclonal antibodies (mAbs) for 30 min at 4°C in the dark. The mAbs used were the following: anti-CD44, -CD45, -CD73, -CD90, -CD105, HLA-ABC (BD Biosciences). Stained cells were analyzed by flow cytometry using a FACS (BD Biosciences) and data were analyzed using FlowJo software (Tree Star) for data management. Cells were electronically gated according to light-scattering properties to discriminate cell debris. Isotype-matched non-specific antibodies were used as the negative control.

**Cell Viability Assay.** To evaluate cell viability, hBM-MSCs were seeded on different substrates PSU, PSU+$O_2$, PSU+a-C:H, and patterned PSU+$O_2$+a-C:H at a starting concentration of 2 × $10^3$ cells $mL^{-1}$ of control medium. At different times (3, 7, and 14 days), cell viability was measured by assaying the mitochondrial dehydrogenase activity through the XTT salt solution (Sigma) assay for 4 h at 37°C according to the manufacturer's recommendations. The absorbance of the samples was measured using a microtiter plate reader (GDV) at 450 nm with a reference wavelength at 650 nm.

**Immunofluorescence.** Immunofluorescence images were performed as previously described[23]; briefly, cells were rinsed twice with PBS, fixed in 4% paraformaldheyde for 30 min and, after PBS washing, cells were permeabilized, blocked (PBS+10% FBS, 0.1% Triton X-100) for 1 h at RT, and incubated with phalloidin (Alexa-fluor-488 phalloidin, Invitrogen), for 20 min then further incubated overnight at 4°C with other primary antibodies: anti-α-tubulin (Santa-Cruz Biotechnology). After being washed with PBS and stained with Alexa-Fluor 594-nm conjugated secondary antibodies (Invitrogen) for 1 h at room temperature, samples were mounted, and nuclei were counterstained with Vectashield with DAPI (Vector Laboratories). Images were acquired using fluorescence microscopy (Eclipse-TE2000-S, Nikon) using the F-ViewII FireWire camera (Soft Imaging System, Olympus).

**Cell Alignment and Elongation Factor.** Cell alignment and Elongation Factor was evaluated on cells cultured on each substrate at days 3 and 7. Eight different areas were photographed (20× magnification)[23,24] and an average of 300 cells was analyzed. Images were acquired using fluorescence microscopy (Eclipse-TE2000-S, Nikon) using the F-ViewII FireWire camera (Soft Imaging System, Olympus). The *E* factor is defined as the ratio between long and short axis minus 1. Thus, $E = 0$ for a circle, and $E = 1$ for an ellipse with an axis ratio of 0.5.[24] Cells were considered aligned if the angle between the long axis and the grating was <15°. Results are expressed as percentage of cell alignment compared with the cell nuclei.

## RESULTS AND DISCUSSION

### Polymeric Surface Nanotopography

The spin coated PS films show uniform morphology, transparency and a regular thickness of 18 μm, as measured by FESEM stratigraphy and reflection optical microscope (images do not show). An efficient system was developed to design and produce nanostructured surfaces and micropatterns having various morphology, shape and dimensions on polystyrene substrates. The Oxygen plasma treatments induce changes in the physical–chemical surface characteristics of polymeric films.

Figure 1 shows FESEM and AFM images of the Oxygen plasma treated PS surface for 20 min at 20 W power supply, compared to the untreated PS FESEM images [Figure 1(a)]: micropatterned PS surface (b), FESEM nanotopography induced by Oxygen gas (c), underlining the morphological changes occurred to

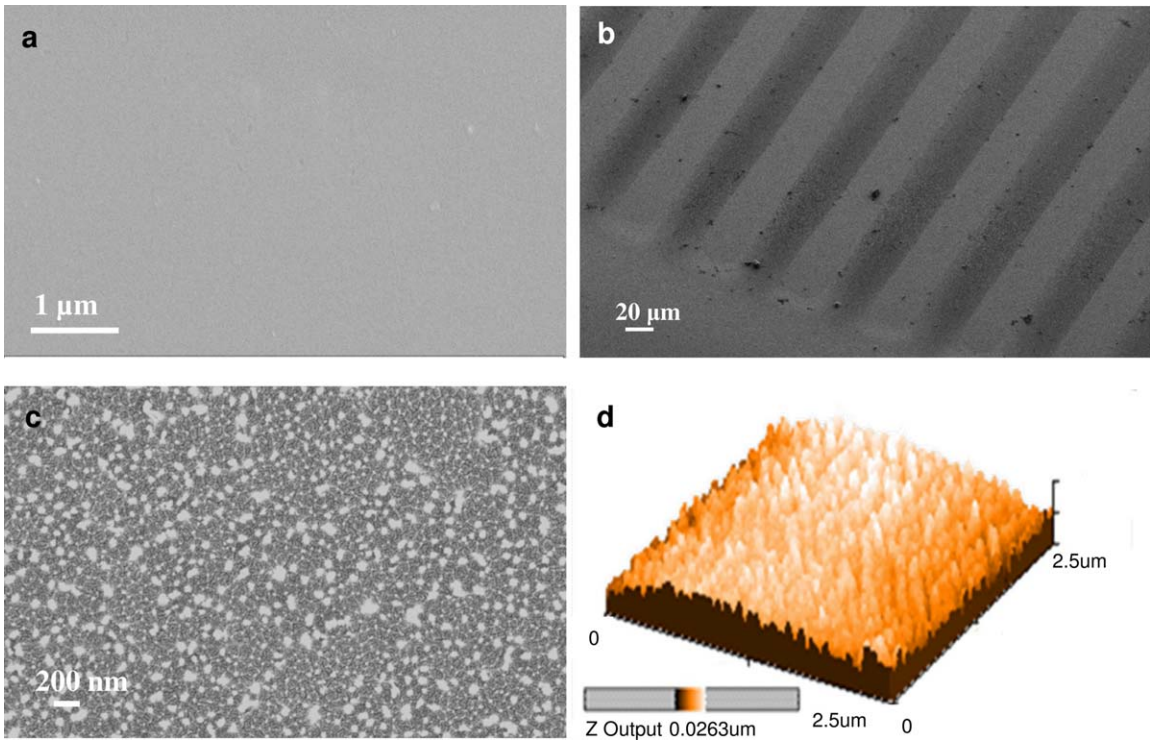


**Figure 1.** FESEM images of pristine polystyrene film (a), Oxygen plasma treated PS films: patterned grooves (b) and nanostructured PS surface. AFM image of nanostructured Oxygen treated PS surface. [Color figure can be viewed in the online issue, which is available at wileyonlinelibrary.com.]

the PS surface after treatment (c). Figure 1(b) shows the morphology of the patterned film, the grooves exposed to the plasma were etched. The region not covered by the mask and exposed to the plasma treatment results well define, with a clear border. The pattern dimension obtained was 40 μm groove width and 30 μm spacing. The etching effect of the treatment was revealed by the introduction of a regular nano-dome structure with uniform distribution, with a clearly increase in surface roughness [Figure 1(c,d)]. The AFM image [Figure 1(d)] confirms the nanodome structure, with a height less of 5 nm.

Figure 2 shows AFM profile and 3D images of nanopatterned PS films obtained by using Oxygen gas, 20 W power supply and different treatment time (5, 10, 20, and 30 min), in order to study ridge thickness and the steep of the transition. The profile of the ridge is clear, it is evident the etching effect of plasma treatment. Figure 3 shows step thickness measured by AFM for sample treated with Oxygen at different power for different time. By using 10 W power supply ridge heights ranging from 50 to 280 nm were obtained, with 20 W ridge heights vary from 140 nm for 5 min to 1100 nm for 30 min, finally for treatments at 30 W were measured step of 240 nm for 5 min and 1800 nm for 30 min of treatment. Hence using plasma treatment were produced nanostructured surfaces with hydrophilic grooves and hydrophobic ridges. In fact static contact angle measurements were performed to study the plasma treatment effects on wettability and surface energy. Contact angle measurements are one of the simplest methods to determine changes that take place in the very outer layer of materials during their surface treatment. Figure 4 shows water contact angle (WCA) values and images of pristine and $O_2$ plasma treated PS surfaces. The PSU film shows a relatively hydrophobic behavior with a water contact angle of 90°, as reported in literature.[25] WCA decreases with increasing the power supply and the treatment times. The value decreased dramatically within a very short time of Oxygen plasma treatment, for 2.5 min of treatment the contact angle ranging from 34° for a power of 5 W to a value that is <10° for 30 W, was obtained the same trend for the treatments of 5 min, from 27° for 5 W to <10° for 20 and 30 W, and treatments of 10 min, from 16° for 5 W, 13 for 10 W to <10° for 20 and 30 W. The value decreases more rapidly as increases the power, it reached value <10° for 5 min of treatment at 20 and 30 W.

The hydrophilicity was measured not only by contact angle but also by surface energy, the change in free surface energy was studied. Table I reports the values of water and diiodomethane contact angle used to calculate the surface energy[21] in its disperse and polar components.

It was reported[26] that good cell spreading only occurred when was higher than ~57 mN $m^{-1}$ so the oxygen treatments make the surface very hydrophilic and presumably suitable for cell cultures, raising the surface energy from 48.11 mN $m^{-1}$ for the untreated PS to 80.79 mN $m^{-1}$ for a treatment at 20 W for 5 min.

Figure 5 shows FTIR–ATR spectra of pristine polystyrene film (PSU), oxygen treated and PS+a-C:H, in the 3800–2500 $cm^{-1}$ (a) and 2000–700 $cm^{-1}$ (b). The FT-IR spectra of PSU displays the typical characteristics absorption bands of the polymer, underling that the plasma treatments do not modify the carbonyl peak. The Oxygen plasma treated polystyrene film shows the peak at 1746 $cm^{-1}$ that corresponds to C═O stretching,

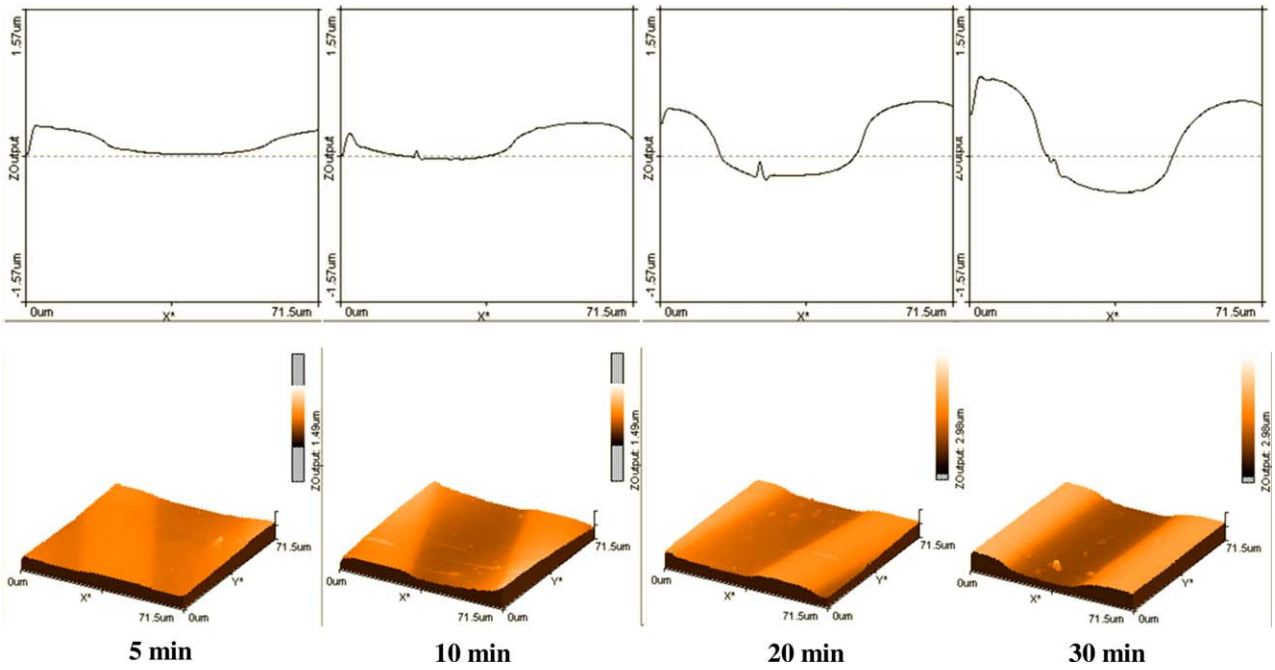


**Figure 2.** AFM profile and 3D images of nanopatterned PS by using Oxygen plasma treatment, 20 W and different treated times (5, 10, 20, and 30 min). [Color figure can be viewed in the online issue, which is available at wileyonlinelibrary.com.]

which indicates the reaction of oxygen plasma with the PS to form a C═O group on the surface. This effect is responsible for the decrease in the contact angle. Meichsner et al. observed bands at 3500–3000 $cm^{-1}$ and various C—O bands (1300–1000 $cm^{-1}$), which are similar to our observations.[27]

It is well known that an oxygen plasma can react with the polymer surface to produce a variety of atomic oxygen functional groups, including C—O, C═O, O—C═O, and $CO_3$ at the surface. In an oxygen plasma, two processes occur simultaneously, etching of the polymer surface through the reaction of atomic oxygen with the surface carbon atom, giving volatile reaction products and the other one is the formation of oxygen functional groups at the polymer surface through the interaction between the active species from the plasma and the surface atom.[28] The balance of these two processes depends on the operation of a given process.[29]

### PS/a-C:H Bilayer Films

Amorphous carbon film was uniformly deposited on polystyrene substrate.

The amorphous carbon (a-C:H) film covers regularly the polystyrene film, hence the double layer of PSU+a-C:H has the chemical properties of amorphous carbon since the PECVD parameters permit a uniform and regular deposition of about 30 nm on polymeric substrate.[23]

The a-C:H coating show a good stability and adhesion on PS, in water at 37°C, the conditions were selected in order to simulate the physiological environment.

Uniform double layer system has the surface characteristic of amorphous carbon,[23] with a contact angle of 77° and surface free energy of 51.15 mN $m^{-1}$.

The infrared spectrum of PSU+a-C:H film [Figure 5(a,b)] shows the presence of infrared peaks such as alkyne end groups and C═C bonds. The creation of alkyne end groups (R—C—C—H) is evidenced by the new band at 3300 $cm^{-1}$, which is assigned to C—H stretching vibration mode of the alkyne end group. Large peaks are seen at 1630 $cm^{-1}$ due to C═C ($sp^2$ bonding). The intensity of the peaks assigned to $sp^3$ $CH_2$ and $sp^3$ $CH_3$ at around 2850–2950 $cm^{-1}$ is increased. This result suggests that this surface coating is mostly contained in a mixture of $sp^2$, $sp^3$, and few $sp^1$ coordinated carbon atoms in a

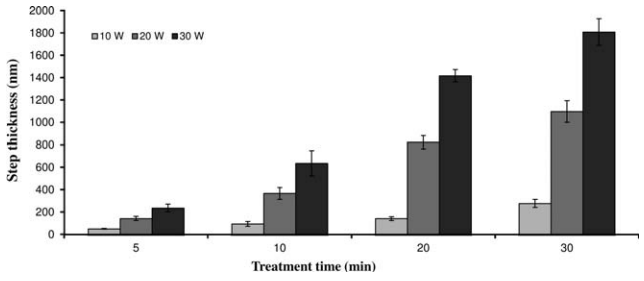


**Figure 3.** Evolution with plasma treatment parameters of step thickness.

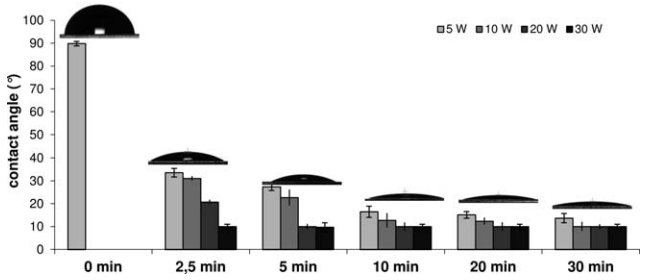


**Figure 4.** Water contact angle representative images and data of untreated and oxygen plasma treated PS.

**Table I.** Contact Angle Values, Surface Energy, Polar, and Dispersive Components of PSU, PSU+$O_2$, and PSU+a-C:H

| Samples | Process parameters (gas, power supply, time) | C.A. $H_2O$ (°) | C.A. $CH_2I_2$ (°) | S.E. (mN $m^{-1}$) | disp. (mN $m^{-1}$) | Polar (mN $m^{-1}$) |
|---|---|---|---|---|---|---|
| PSU | - | 90 | 20 | 48.11 | 47.75 | 0.36 |
| PSU+$O_2$ | $O_2$, 5 W, 5 min | 27 | 23 | 73.37 | 46.81 | 26.56 |
| PSU+$O_2$ | $O_2$, 20 W, 5 min | 8 | 3 | 80.79 | 50.71 | 30.08 |
| PSU+a-C:H | $CH_4$, 15 W, 5 min | 77 | 19 | 51.15 | 48.16 | 2.99 |

disordered network. Furthermore in the ATR spectrum of PS+a-C:H films the peaks corresponding to the aromatic vibration in PS decrease the intensity and they are replaced by the alkene C=C peak at 1670 $cm^{-1}$.

Figure 6 shows the nanomechanical properties of PSU and PSU+a-C:H films. Representative load-displacement plots of film indentation and representative optical image of indentation are shown in Figure 5(a). In these plots lower indentation depths indicate higher hardness, while higher slopes of unloading curve indicate high stiffness or elastic modulus of the samples. PSU film exhibits higher indentation depth and unloading slope compared to PSU+a-C:H. These data were used to calculate the hardness and the reduced modulus of films by using Oliver&Pharr method.[30] All nanomechanical data were reported in Table II. The maximum depth in PSU film indentation is about 900 nm which is <1/10 of film thickness, indicating that the sample holder effect may thus be neglected.[31] The PSU film exhibits a hardness of about 0.29 GPa and reduced elastic modulus of 12.2 GPa, PSU+a-C:H is harder (1 GPa) but displays a lower modulus (3.9 GPa). It is evident that the data reported for PSU+a-C:H are not representative of the amorphous carbon coating, but the obtained elastic modulus value could be attributed to whole bi-layer configuration, since the modulus of amorphous carbon film is usually higher, as previously reported.[32] Because of the low a-C:H thickness (30 nm), the role of film/substrate interface have to be taken into consideration, in elastic modulus measurements, while the friction coefficient values are not affected by the mechanical properties of the substrate, but only the outmost layer. Because continuous curves are observed during unloading stage no severe failure occurs during the loading process.[11] Figure 6(b) shows the friction coefficient curve measured at constant load of 5 mN that decreases from 0.76 for PSU to 0.17 for PSU+a-C:H. Moreover the amorphous carbon coating shows good adhesion with the polymeric film since the onset of cracking or delamination of a hard coating is signalled by a sudden increase in friction coefficient.[33,34] The plots reported in Figure 6(b) show flat behavior of the friction coefficient as a function of the scan distance, it should be noted that there is data scattering in the friction coefficient of PSU while PSU+a-C:H exhibits constant results. This effect could be due to the nanoscale topography and surface structures of the analyzed films.[31] Furthermore it is well known that the mechanical properties of the surface have important implications in stem cell behavior, as previously reported,[35–37] since stem cells are able to convert mechanical cues on biochemical signals and in turn modulate their fate. Figure 7 shows the protein adsorption of each substrate. After 30 min of adsorption, we found comparable quantity of purified BSA, FBS

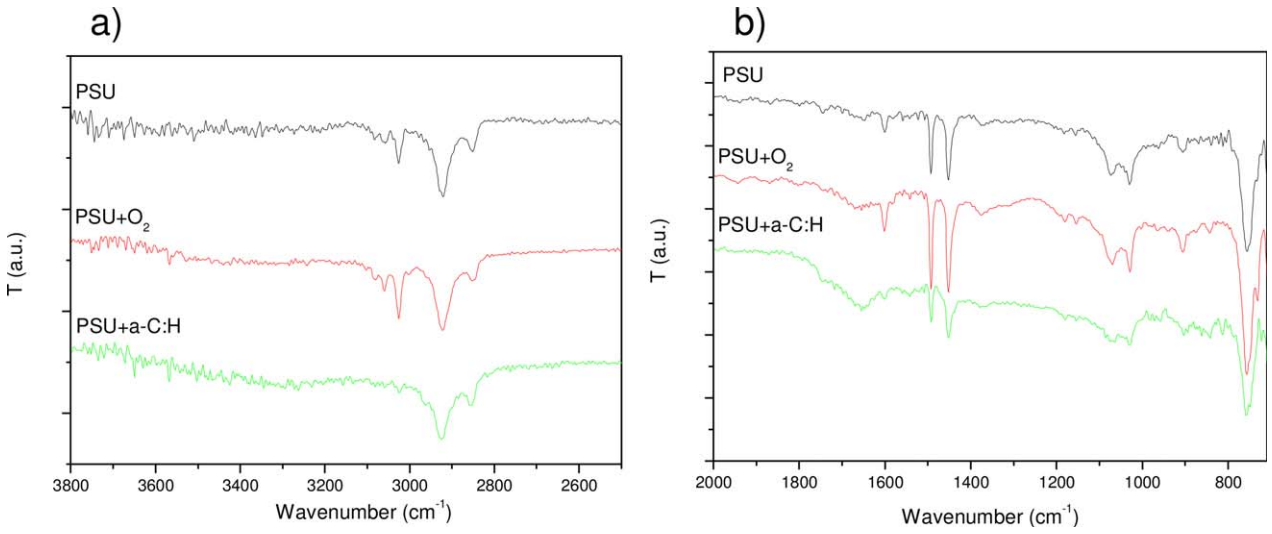


**Figure 5.** FTIR–ATR spectra of pristine polystyrene film (PSU), Oxygen treated and PS+a-C:H, in the 3800–2500 $cm^{-1}$ (a) and 2000–700 $cm^{-1}$ (b). [Color figure can be viewed in the online issue, which is available at wileyonlinelibrary.com.]

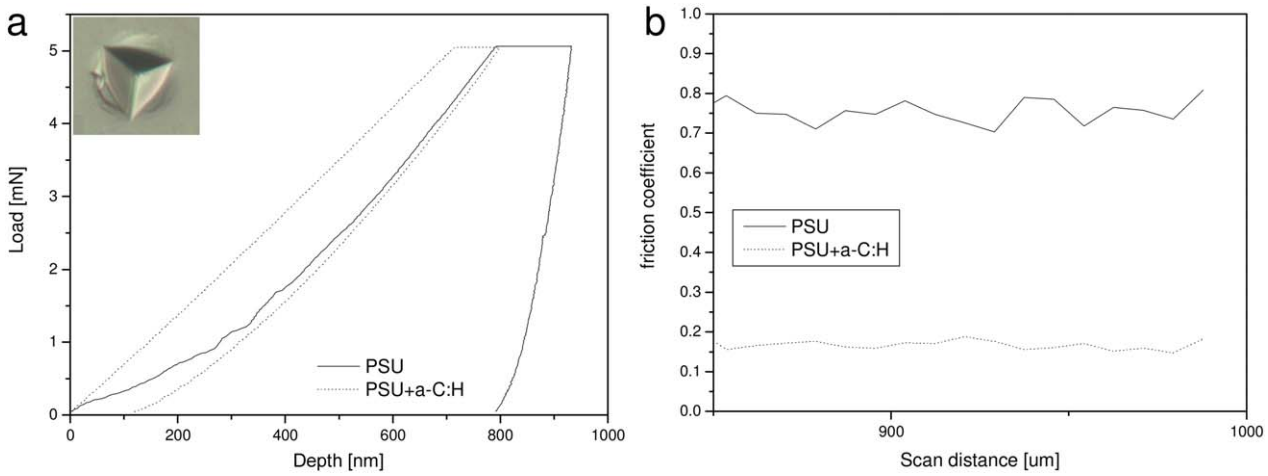


**Figure 6.** Nanomechanical tests of PSU and PSU+a-C:H films. (a) Representative load–unload curves and indentation image; (b) friction coefficient as a function of scan distance. [Color figure can be viewed in the online issue, which is available at wileyonlinelibrary.com.]

10% and plasma between polymers indicating the absence of the influence of surface characteristic of polymers. These results were confirmed in all polymers after 24 h for FBS 10% and pure BSA, although levels of this protein were highest. Interestingly levels of plasma adsorbed were dissimilar between polymers reaching the highest value on $O_2$ treated surface.

### Biological Evaluation

To assess the coating cytocompatibility, we cultured hBM-MSCs on each substrate (PSU, PSU+$O_2$, PSU+a-C:H, and patterned PS+$O_2$+a-C:H). Figure 8(a) shows a schematic view of the surface structures on glass coverslip substrate: uniform, Oxygen treated PS, and double layer PS-amorphous carbon thin films together [Figure 8(b)] with representative images of stem cells after culture and F-actin immune-staining. Figure 8(c) shows the measures of the cell density, cellular length and width, cell area after 3 and 7 days of culture on each coating. As control stem cells were cultured on TCP. We observed a comparable viability and absence of toxic signs on stem cells cultured on each substrate and TCP (data not shown), whereas we found significant differences on stem cell behavior perhaps as consequence of the characteristic of each coating (Figures 7 and 8). hBM-MSCs seeded on PSU showed the lowest values of cell density, cellular length and width, cell area indicating differences in morphology and spreading capabilities as also emerge from the related cell cytoskeleton images [Figure 8(a,b)]. Conversely, hBM-MSCs seeded on PSU+$O_2$ or PSU+a-C:H showed cellular distension comparable to that routinely observed on TCP substrates [Figure 8(a)], but revealed cell parameters almost two fold higher than those evaluated on PSU [Figure 8(b)]. Confirming our previous observation[17,23] hBM-MSCs seeded on PSU+$O_2$+a-C:H with groove pattern, aligned along the pattern direction [Figure 9(a)].

As showed in Figure 9, the F-actin fibers [Figure 9(b)] and α -tubulin [Figure 8(c)] aligned along the direction of the a-C:H grooves indicating a direct effect of the nanoconfiguration on the change of the cytoskeleton organization. We monitored a

**Table II.** Hardness, Reduced Modulus, and Friction Coefficient of Polystyrene and a-C:H Deposited on PS

| Sample | H (Gpa) | Er (Gpa) | Friction coefficient |
|---|---|---|---|
| PSU | 0.29 ± 0.02 | 12.2 ± 0.6 | 0.76 ± 0.04 |
| PSU+a-C:H | 1.0 ± 0.1 | 3.9 ± 0.2 | 0.17 ± 0.02 |

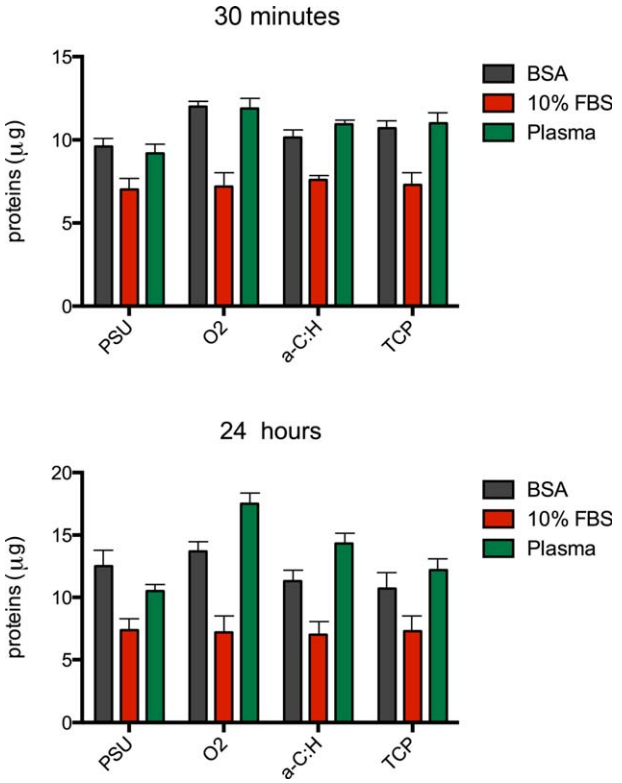


**Figure 7.** Protein adsorption measurements of PSU, PSU+$O_2$ and PSU+a-C:H, at 30 min and 24 h. Protein adsorption is expressed as µg of total proteins bonded to the polymer. [Color figure can be viewed in the online issue, which is available at wileyonlinelibrary.com.]

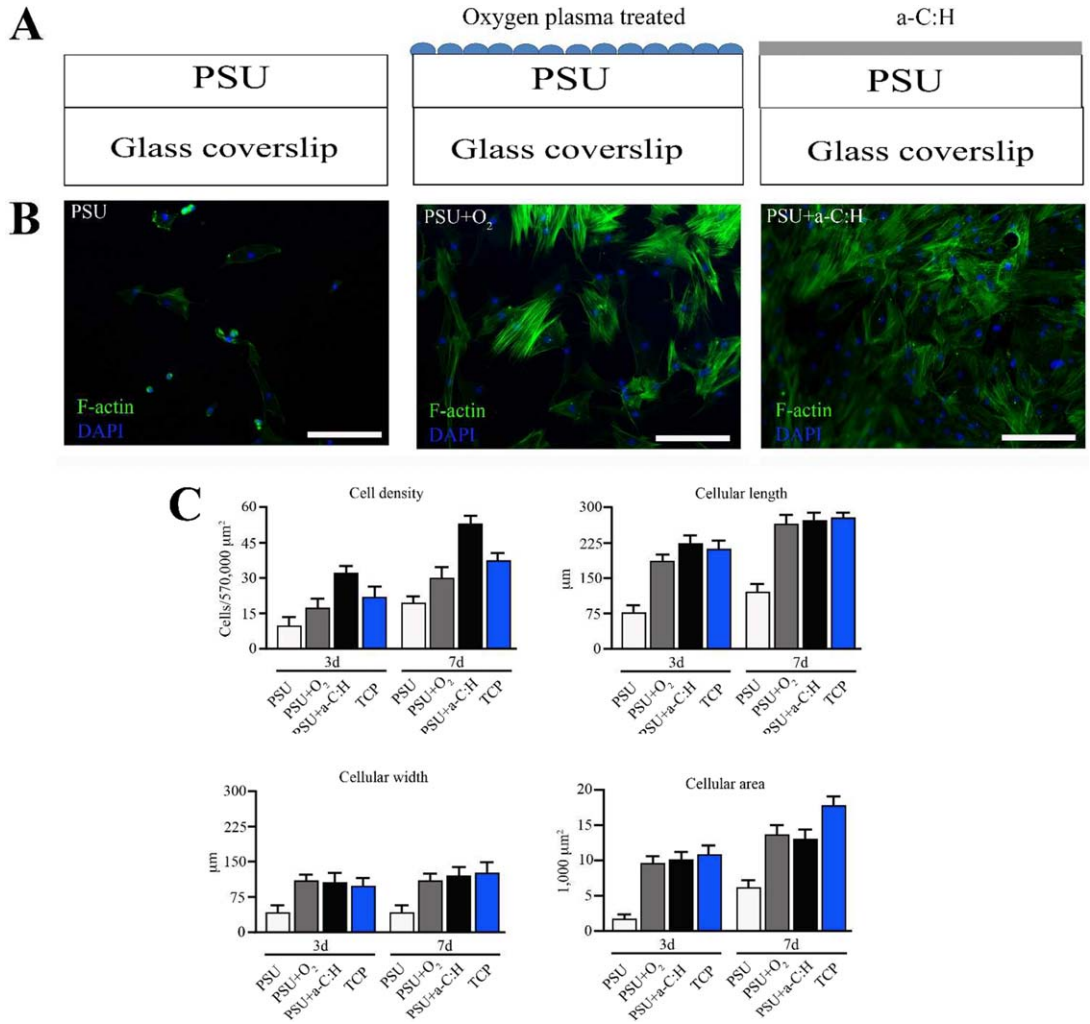


**Figure 8.** (A) scheme of plasma modifications. (B) Representative images of hBM-MSCs seeded on each corresponding surface polymer. (C) Measures of the cell density, cellular length and width, cell area after 3 and 7 days of culture on each coating (see Method section for experimental details). [Color figure can be viewed in the online issue, which is available at wileyonlinelibrary.com.]

cell alignment of 71% higher with respect to uniform surfaces (PSU, PSU+$O_2$ and PSU+a-C:H) [Figure 9(d)] and comparable aligned level to that measured in nanopatterned a-C:H in our previous work.[17] Alignment of hBM-MSCs cultured was also observed on patterned PSU (Table III) although in a lesser extent compared to PSU+$O_2$+a-C:H. Interestingly comparing stem cell grown on both ridges PSU+$O_2$+a-C:H and PSU revealed that elongation factor values varied with power supply and treatment time, that are parameters necessary for a fine modulation of the step grooves and the surface roughness (Table III). These data, according to our previous observation,[17,23,35,36] indicated that the structure of the substrate and the type of modifications influence the cell morphology.

The overall data indicated that PSU, PSU+$O_2$, PSU+a-C:H and patterned PSU+$O_2$+a-C:H are suitable substrates for h-BM-MSCs, but: (i) PSU+$O_2$, PSU+a-C:H coatings preserve the stem cell behavior observed on routinely used TCP: (ii) PSU influences the size, adhesion and stem cell spreading; (iii) patterned PS+$O_2$+a-C:H forced hBM-MSCs to spread along the grating leading an elongated cellular morphology. Finally these results confirm our previous observation[17,23,35,36] that the substrate modifications could influence the cell morphology.

## CONCLUSIONS

The utility of the micropatterns on polymers for tissue culture applications have clearly been demonstrated by the stem cell culture. Therefore, the wrinkled surface combined with amorphous carbon films would possess biological compatibility and may have the potential for a vast range of biomedical applications.

In summary top-down processing approach, using combination of plasma etching and deposition techniques permits the development of large nanopatterned surfaces.

We have highlighted some of the surface topographies of PS polymer created by using plasma technique. Various surface topographies such as groove, nanodome can be easily created by the technique and the control of the plasma parameters directly affects the surface topographies. The interaction of human bone marrow stem cells with specific designed topography has proven

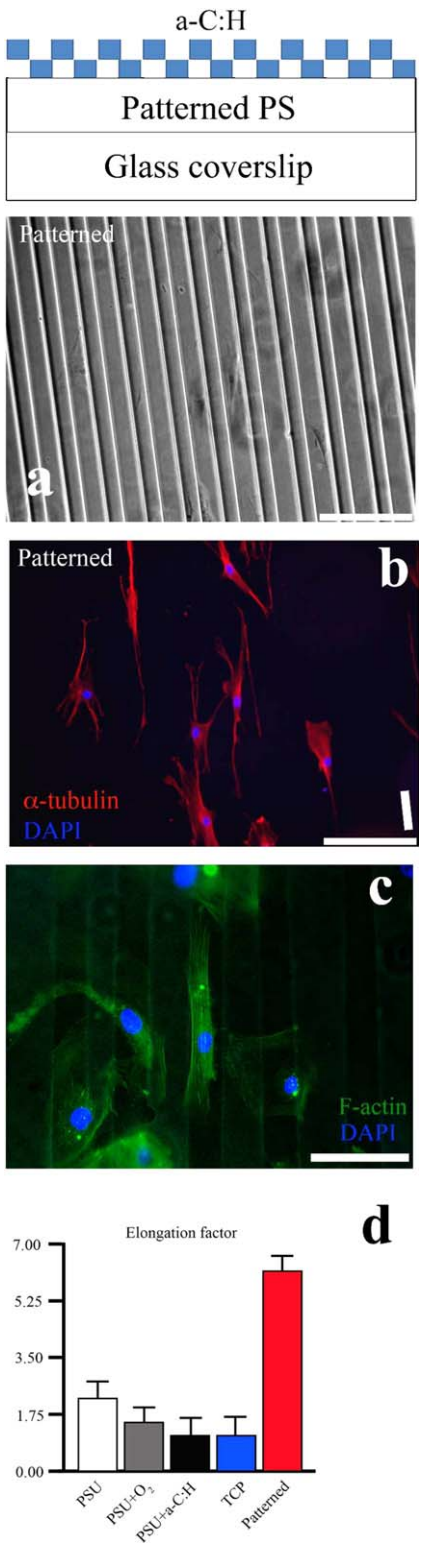


**Figure 9.** Representative images of hBM-MSCs seeded on patterned a-C:H/PS (a). (b) a-Tubulin (RED), (c) F-Actin (GREEN) nuclei (DAPI). (d) Measurement of Elongation Factor on patterned and uniform coatings (see Results section for details). [Color figure can be viewed in the online issue, which is available at wileyonlinelibrary.com.]

**Table III.** Elongation Factor and Alignment Percentage of Uniform and Patterned Surfaces Developed by Using Different Plasma Process Parameters (Time and Power Supply), that Permit to Obtain Groove with Different Step Thickness

| Treatment parameters (power supply, time) | Step thickness (nm) | PSU | | PSU+a-C:H | |
|---|---|---|---|---|---|
| | | *E* | %All | *E* | %All |
| 10 W, 10 min | 9 | 2.4 | 20 | 1.9 | 7 |
| 30 W, 5 min | 240 | 3.5 | 8 | 5.6 | 3 |
| 30 W, 10 min | 640 | 1.9 | 9 | 3.3 | 8 |
| 30 W, 20 min | 1420 | 5.6 | 30 | 5.2 | 27 |
| 30 W, 30 min | 1800 | 3.4 | 45 | 6.3 | 71 |

to be an important signaling modality in controlling cell function.

Surface modification using plasma methods has a vast range of applications; therefore, it is crucial for materials scientists, biologists and medical doctors to firmly collaborate and seek to understand how the local interactions between cells and their surrounding microenvironment can regulate cellular behavior in order to develop highly functionalized scaffolds for tissue engineering applications.

This study was supported by the *Fondazione Cassa di Risparmio di Perugia, Italy* (grant no. 2010,0110445 to S.M.),

## REFERENCES

1. Armentano, I.; Ciapetti, G.; Pennacchi, M.; Dottori, M.; Devescovi, V.; Granchi, D.; Baldini, N.; Olalde, B.; Jurado, M. J.; Alava, J. I. M.; Kenny, J. M. *J. Appl. Polym. Sci.* **2009**, *114*, 3602.
2. Vitte, J.; Benoliel, A. M.; Pierres, A.; Bongrand, P. *Eur. Cells Mater.* **2004**, *7*, 52.
3. Armentano, I.; Bitinis, N.; Fortunati, E.; Mattioli, S.; Rescignano, N.; Verdejo, R.; Lopez-Manchado, M. A.; Kenny, J. M. *Prog. Polym. Sci.* **2013**, *38*, 1720.
4. Wende, K.; Schroeder, K.; Lindequist, U.; Ohl, A. *Plasma Processes Polym.* **2006**, *3*, 524.
5. Kontziampasis, D.; Constantoudis, V.; Gogolides, E. *Plasma Processes Polym.* **2012**, *9*, 866.
6. Chan, C. M.; Ko, T. M.; Hiraoka, H. *Surf. Sci. Rep.* **1996**, *24*, 3.
7. Ong, S.-E.; Zhang, S.; Du, H.; Wang, Y.; Ma, L.-L. *Thin Solid Films* **2008**, *516*, 5152.
8. Salgueiredo, E.; Vila, M.; Silva, M. A.; Lopes, M. A.; Santos, J. D.; Costa, F. M.; Silva, R. F.; Gomes, P. S.; Fernandes, M. H. *Diamond Relat. Mater.* **2008**, *17*, 878.
9. Roy, R. K.; Lee, K.-R. *J. Biomed. Mater. Res. B Appl. Biomater.* **2007**, *83B*, 72.
10. Bociaga, D.; Mitura, K. *Diamond Relat. Mater.* **2008**, *17*, 1410.
11. Wang, H.; Xu, M.; Zhang, W.; Kwok, D. T. K.; Jiang, J.; Wu, Z.; Chu, P. K. *Biomaterials* **2010**, *31*, 8181.

12. Ni, M.; Tong, W. H.; Choudhury, D.; Rahim, N. A. A.; Iliescu, C.; Yu, H. *Int. J. Mol. Sci.* **2009**, *10*, 5411.
13. Clark, P.; Connolly, P.; Curtis, A. S. G.; Dow, J. A. T.; Wilkinson, C. D. W. *Development* **1990**, *108*, 635.
14. Lee, H.-U.; Jeong, Y.-S.; Jeong, S.-Y.; Park, S.-Y.; Bae, J.-S.; Kim, H.-G.; Cho, C.-R. *Appl. Surf. Sci.* **2008**, *254*, 5700.
15. Tunma, S.; Song, D.-H.; Kim, S.-E.; Kim, K.-N.; Han, J.-G.; Boonyawan, D. *Appl. Surf. Sci.* **2013**, *283*, 930.
16. Dalby, M. J.; Gadegaard, N.; Curtis, A. S. G.; Oreffo, R. O. C. *Curr. Stem Cell Res. Ther.* **2007**, *2*, 129.
17. D'Angelo, F.; Armentano, I.; Mattioli, S.; Crispoltoni, L.; Tiribuzi, R.; Cerulli, G. G.; Palmerini, C. A.; Kenny, J. M.; Martino, S.; Orlacchio, A. *Eur. Cells Mater.* **2010**, *20*, 231.
18. Recknor, J. B.; Recknor, J. C.; Sakaguchi, D. S.; Mallapragadaa, S. K. *Biomaterials* **2004**, *25*, 2753.
19. Zhu, B. S.; Zhang, Q. Q.; Lu, Q. H.; Xu, Y. H.; Yin, J.; Hu, J.; Wang, Z. *Biomaterials* **2004**, *25*, 4215.
20. Kondyurin, A.; Gan, B. K.; Bilek, M. M. M.; Mizuno, K.; McKenzie, D. R. *Nucl. Instrum. Methods Phys. Res. Sect. B Beam Interactions Mater. Atoms* **2006**, *251*, 413.
21. Owens, D. K.; Wendt, R. C. *J. Appl. Polym. Sci.* **1969**, *13*, 1741.
22. Bradford, M. M. *Anal. Biochem.* **1976**, *72*, 248.
23. Martino, S.; D'Angelo, F.; Armentano, I.; Tiribuzi, R.; Pennacchi, M.; Dottori, M.; Mattioli, S.; Caraffa, A.; Cerulli, G. G.; Kenny, J. M.; Orlacchio, A. *Tissue Eng. A* **2009**, *15*, 3139.
24. Yim, E. K. F.; Pang, S. W.; Leong, K. W. *Exp. Cell Res.* **2007**, *313*, 1820.
25. Zhao, Y.; Tang, S.; Myung, S. W.; Lu, N.; Choi, H. S. *Polym. Test.* **2006**, *25*, 327.
26. Schakenraad, J. M.; Busscher, H. J.; Wildevuur, C. R. H.; Arends, J. *J. Biomed. Mater. Res.* **1986**, *20*, 773.
27. Meichsner, J.; Zeuner, M.; Kramers, B.; Nitschke, M.; Rochotzki, R.; Barucki, K. *Surf. Coat. Technol.* **1998**, *98*, 1565.
28. Morra, M.; Occhiello, E.; Garbassi, F. *Surf. Interface Anal.* **1990**, *16*, 412.
29. Guruvenket, S.; Mohan R. G.; Komath, M.; Raichur, A. M. *Appl. Surf. Sci.* **2004**, *236*, 278.
30. Oliver, W. C.; Pharr, G. M. *J. Mater. Res.* **1992**, *7*, 1564.
31. Lee, J. W.; Duh, J. G. *Surf. Coat. Technol.* **2004**, *188*, 655.
32. Bhushan, B.; Gupta, B. K.; Azarian, M. H. *Wear* **1995**, *181*, 743.
33. Wei, G.; Scharf, T. W.; Zhou, J. N.; Huang, F.; Weaver, M. L.; Barnard, J. A. *Surf. Coat Technol.* **2001**, *146*, 357.
34. Charitidis, C. A. *Int. J. Refractory Metals Hard Mater.* **2010**, *28*, 51.
35. D'Angelo, F.; Armentano, I.; Cacciotti, I.; Tiribuzi, R.; Quattrocelli, M.; Del Gaudio, C.; Fortunati, E.; Saino, E.; Caraffa, A.; Cerulli, G. G.; Visai, L.; Maria Kenny, J.; Sampaolesi, M.; Bianco, A.; Martino, S.; Orlacchio, A. *Biomacromolecules* **2012**, *13*, 1350.
36. Martino, S.; D'Angelo, F.; Armentano, I.; Maria Kenny, J.; Orlacchio, A. *Biotechnol. Adv.* **2012**, *30*, 338.
37. Engler, A. J.; Sen, S.; Sweeney, H. L.; Discher, D. E. *Cell* **2006**, *126*, 677.